Journal of Power Sources 268 (2014) 718–727

Contents lists available at ScienceDirect

Journal of Power Sources

journal homepage: www.elsevier.com/locate/jpowsour

New latent heat storage system with nanoparticles for thermal management of electric vehicles

N. Javani [a, *], I. Dincer [a], G.F. Naterer [b]

[a] Faculty of Engineering and Applied Science, University of Ontario Institute of Technology, 2000 Simcoe St. North, Oshawa, ON L1H 7K4, Canada
[b] Faculty of Engineering and Applied Science, Memorial University of Newfoundland, 240 Prince Phillip Drive, St. John's, NL A1B 3X5, Canada

HIGHLIGHTS

- A new passive thermal management system is developed for electric vehicles.
- Thermal conductivity of PCM in storage systems is improved by introducing carbon nanotubes.
- Energy storage dimensions are optimized to be applicable to an electric vehicle TMS.
- The placement of carbon nanotubes in PCM improves the bulk thermal conductivity.

ARTICLE INFO

Article history:
Received 15 March 2014
Received in revised form
18 June 2014
Accepted 19 June 2014
Available online 26 June 2014

Keywords:
Thermal management
Heat exchanger
Electric vehicle
Carbon nanotube
Phase change material
Optimization

ABSTRACT

In this paper, a new passive thermal management system for electric vehicles is developed. A latent heat thermal energy storage with nanoparticles is designed and optimized. A genetic algorithm method is employed to minimize the length of the heat exchanger tubes. The results show that even the optimum length of a shell and tube heat exchanger becomes too large to be employed in a vehicle. This is mainly due to the very low thermal conductivity of phase change material (PCM) which fills the shell side of the heat exchanger. A carbon nanotube (CNT) and PCM mixture is then studied where the probability of nanotubes in a series configuration is defined as a deterministic design parameter. Various heat transfer rates, ranging from 300 W to 600 W, are utilized to optimize battery cooling options in the heat exchanger. The optimization results show that smaller tube diameters minimize the heat exchanger length. Furthermore, finned tubes lead to a higher heat exchanger length due to more heat transfer resistance. By increasing the CNT concentration, the optimum length of the heat exchanger decreases and makes the improved thermal management system a more efficient and competitive with air and liquid thermal management systems.

1. Introduction

Vehicular transportation is responsible for approximately 23% of global energy-related greenhouse gas emissions, and its contribution is increasing rapidly [1]. Electric and hybrid electric vehicles (EVs and HEVs) are considered as promising solutions to this problem. Nonetheless, there are still challenges that prevent their widespread commercialization. The battery pack is among the most significant challenges. By providing requirements to satisfy the need for higher power density in EVs, safety and long-term durability turns to significant issues due to potential overheating or thermal runaway under extreme conditions [2]. Therefore, a well-designed thermal management system (TMS) is needed in electric vehicles to control and cool the battery pack and minimize the safety issues. Strategies for effective thermal management are explained elsewhere [3]. Conventional TMSs include active and passive air and liquid cooling systems.

Due to a simpler system than liquid cooling, air cooling systems can be used for specific short-driving range electric vehicles. An improved model for air cooling TMS in an NiMH battery pack is investigated. By decreasing the non-uniformity of air flow among the cells which is mainly due to the large interfaces, the new system can overcome the drawbacks of conventional air cooing systems [4]. In another study, an ambient air circulating system is designed and manufactured to extract the generated heat in the cells through metal-foam based heat exchanger plates. This experimental study shows that by employing more effective technologies, the

* Corresponding author.
E-mail addresses: Nader.Javani@uoit.ca (N. Javani), Ibrahim.Dincer@uoit.ca (I. Dincer), gnaterer@mun.ca (G.F. Naterer).

http://dx.doi.org/10.1016/j.jpowsour.2014.06.107
0378-7753/

consumed power to drive the air can be even lower than the energy consumption of liquid cooling systems [5]. Generally liquid cooling systems need a refrigeration cooling cycle which adds more complexity to the TMS [6]. Furthermore, air cooling systems in active and even passive configurations may fail to provide the cooling load in battery packs in abusive conditions [7,8].

An alternative option in thermal management of electric vehicles is the application of phase change materials (PCMs). The effectiveness of PCMs for thermal management purposes has been studied by various researchers [9,10]. PCMs around the battery pack in single and double layers as well as cell level integration have been studied elsewhere [11,12]. Alternative technologies such as heat pipes and absorption chillers and ejector cooling systems also have been investigated for thermal management of the battery pack in the electric vehicles [13,14]. On the other hand, latent heat thermal energy storage systems (LHTES) can act as a thermal management system by applying a cooling loop. Most interest has been given to shell and tube systems (more than 70% of all studies) and it has been concluded that thermal loss form shell and tube configurations is minimal [15]. Considering the flow pattern, the parallel flow configuration is better than counter-current flow in the sense of charging and discharging time (improved charging/discharging time by about 5%). Due to a shorter time required for charging/discharging, the heat pipe model is recommended for heat exchanger applications. This configuration has a lower heat loss to the ambient [16]. In addition, it was found that most of the engineering systems employ shell and tube technology which is inexpensive and easier to manufacture with lower maintenance costs [17]. For shell and tube heat exchangers, the length/diameter ratio of the cylinder is important. Small ratios are not practically realistic. On the other hand, for larger L/D, there will be a negligible entry length effect which will lead to better performance of the unit [18]. In an experimental study, shell and tube heat exchangers have shown promising performance. This configuration is more appropriate in applications where the volume is limited [19,20].

A PCM is placed in the space between the tubes (shell side). A comprehensive investigation about different PCMs can be found in a study by Sharma et al. [21]. More information about the PCMs, their properties and applications can be found elsewhere [22,23]. The main drawback of PCMs (both organic and inorganic) which decrease the effectiveness of a shell and tube heat exchanger is their low thermal conductivity (0.1–0.6 W m^{-1} K^{-1}). Lower thermal conductivity, in turn, leads to a low rate of charging and discharging processes and limits the potential application of the PCMs in latent heat storage systems [24,25]. Various methods to improve the heat transfer rate can be summarized as employing extended surfaces, multiple PCMs, micro encapsulation of PCM and methods to enhance the thermal conductivity [26]. Javani et al. [27] have studied an LHTES in parallel with the chiller of a HEV and showed that the exergetic efficiency of the system will increase and reduce the total cost of the system. The results are consistent with similar studies where a TMS of active liquid cooling is employed [28].

Carbon Nanotubes (CNT), especially multi-wall carbon nanotubes have specific properties such as a very high axial thermal conductivity. Due to nano-scale effects on the properties of the material, the measurement of thermal conductivity for CNTs has been reported with different values, normally over a wide range. The axial thermal conductivity of CNT is reported theoretically to be as high as 3000 W m^{-1} K^{-1} [29] or even up to 6600 W m^{-1} K^{-1} [30] for individual multiwall CNTs and single-wall CNTs, respectively. The cooling curves are rather typical for *n*-paraffin waxes. At the lower temperature range for the inlet temperature of a heat transfer fluid (HTF), there is a sharp increase in the energy storage time corresponding to an increase in inlet temperature, while for higher temperature ranges, the storage time will not be affected considerably [31]. The composite PCM/CENG thermal conductivity is about 4–70 W m^{-1} K^{-1} compared to 0.2 or 0.3 W m^{-1} K^{-1} for paraffin waxes. This, in turn, decreases the solidification time, and at the same time, reduces the latent heat of fusion of the mixture [32].

Optimization methods are applied in the design of heat exchangers to meet the requirements and satisfy the constraints. Foli et al. [33] maximized the heat transfer rate and minimized the pressure drop in a micro heat exchanger by these two objective functions. Sanaye and Hajabdollahi [34] applied a multi-objective genetic algorithm to optimize the performance of a shell and tube heat exchanger. Other related works can be found elsewhere [35].

In the current research study, a new configuration for passive thermal management is developed for thermal management of electric vehicles. PCM and a carbon Nanoparticle mixture as a latent heat energy storage system is employed in parallel to the existing thermal management system in a vehicle. The specific objectives of this study are stated as follows:

- To develop and analyze a new passive-mode latent heat thermal energy storage system for optimum thermal management in electric vehicles.
- To investigate the operational ranges of the new PCM to be employed in the heat exchanger.
- To improve the thermal conductivity of the PCM by introducing a specific volumetric concentration of carbon nanotubes.
- To define the probability of nanotubes in a series configuration along with their concentration.
- To develop a new correlation from the optimization results for the length and diameter of the shell along with the tube size based on the different mass flow rate and heat transfer rate.
- To optimize the heat exchanger dimensions with respect to the available space in the vehicle using an evolutionary based genetic algorithm method.
- To apply the practical constrains, heat transfer rate of the cooling load, as well as different mass flow rates, and copper tubes, to build the designed and optimized heat exchanger.

2. System description

A mathematical model is developed for a shell and tube heat exchanger with bare and finned straight tubes. The location of a phase change material tank in the liquid TMS is shown in Fig. 1. As Fig. 2 shows, the coolant will flow through the copper tubes and PCM will be located in the shell space. The outer surface of the tank is considered to be insulated. This will lead to an increase in the heat exchanger effectiveness. A thermal conductivity value of 2000 W m^{-1} K^{-1} is considered for carbon nanotubes in the present research study. Effective thermal conductivity mainly depends on the direction of the nanotubes. If they are placed in a series configuration, the effective thermal conductivity increases dramatically. On the other hand, the effective thermal conductivity will possess the minimum value once the nanotubes are in a parallel arrangement.

3. Heat transfer model

A shell and tube heat exchanger model is developed with respect to the PCM thickness and its effect on the convection heat transfer coefficient, variable heat transfer and mass flow rates in the heat exchanger. Furthermore, a model to calculate the effective properties of the PCM and CNT mixture with various nanoparticle concentrations is introduced. Then, an evolutionary based optimization method of a genetic algorithm (GA) is defined with specified objective functions and constraints.

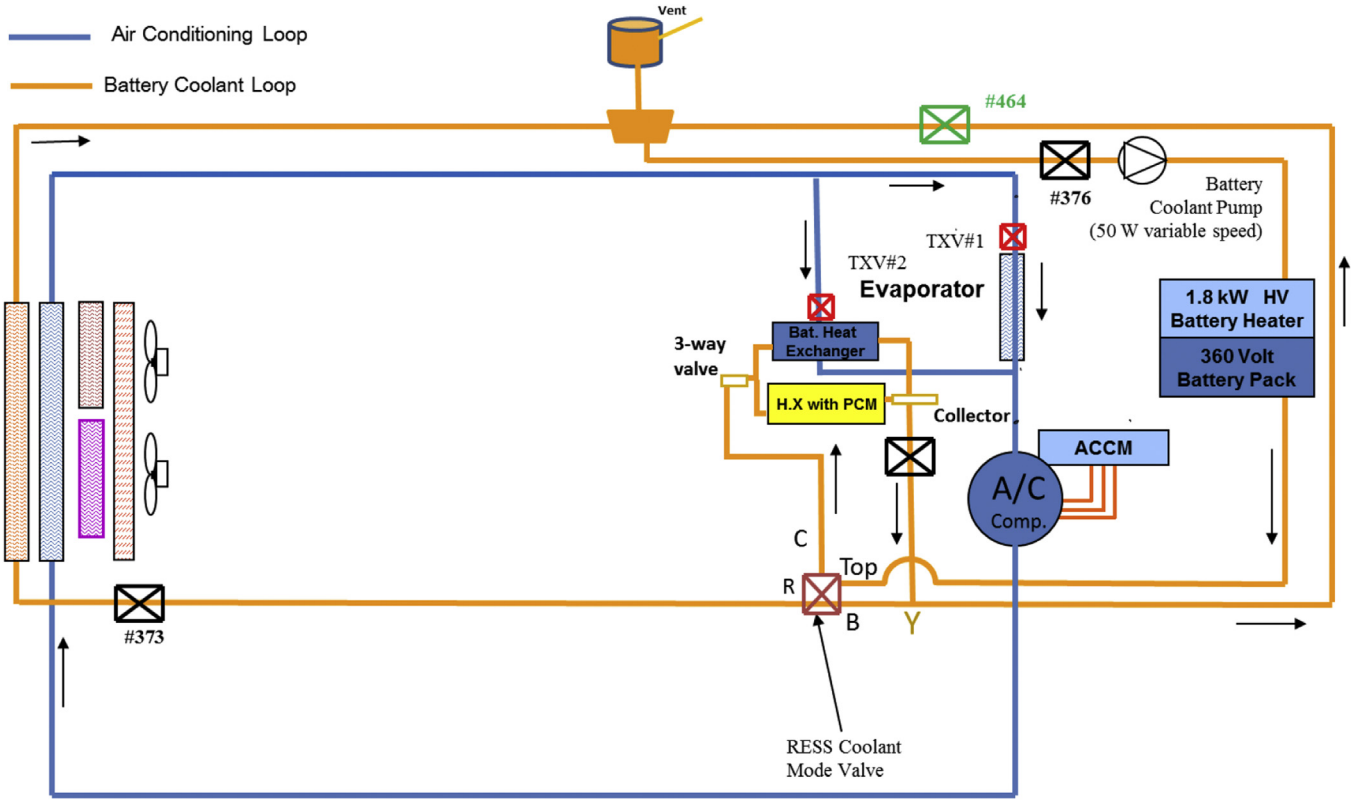

Fig. 1. Simplified representation of the hybrid electric vehicle thermal management system with PCM filled passive heat exchanger.

3.1. Heat transfer coefficients and pressure drops

The LMTD method is applied to predict the heat exchanger performance. The rate of heat transfer is estimated from equation (1) where the logarithmic mean temperature ΔT_{lm} is applied.

$$Q = UA_{\text{tot}}\Delta T_{lm} = (mc_p\Delta T)_h = (mc_p\Delta T)_c \quad (1)$$

$$\Delta T_{lm} = \frac{(T_{h,i} - T_c) - (T_{h,o} - T_c)}{\ln((T_{h,i} - T_c)/(T_{h,o} - T_c))} \quad (2)$$

where A_m is the total heat transfer surface area calculated from:

$$U = \frac{1}{\frac{A_o}{A_i}\frac{1}{h_i} + \frac{1}{\eta_o h_o} + \frac{R_{f,o}}{\eta_o} + \frac{A_o}{A_i}R_{f,i} + A_o R_w} \quad (3)$$

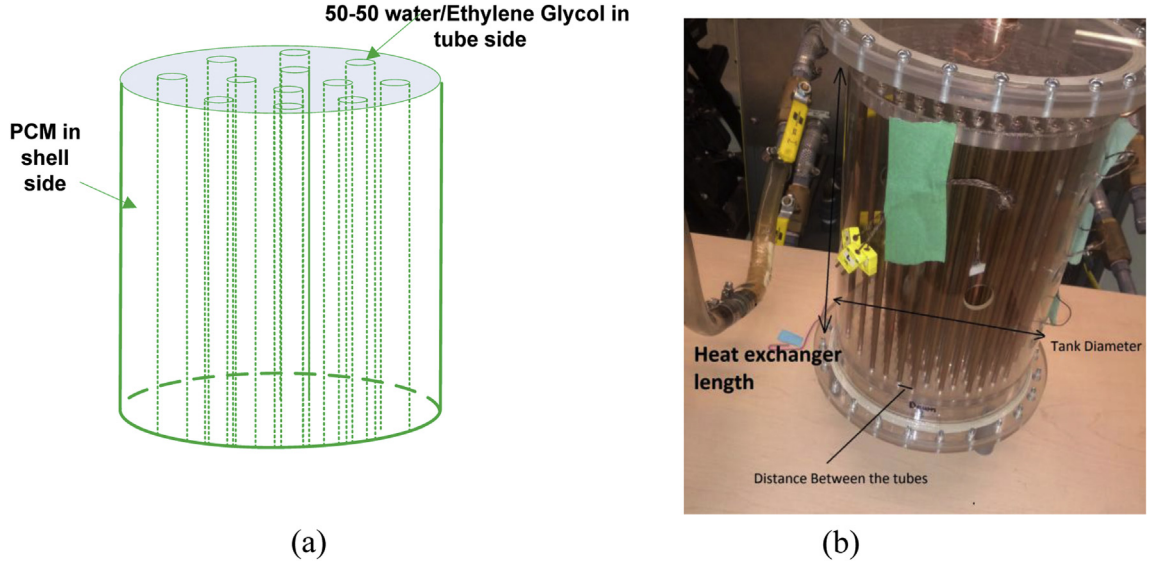

Fig. 2. a) Physical model of heat exchanger, b) optimized and manufactured latent heat thermal energy storage.

$$A_{tot} = A_b + N_f \times s_f \tag{4}$$

$$A_b = \pi d_o N_f \left(s_f - t\right) \tag{5}$$

$$A_i = \pi d_i N_f s_f \tag{6}$$

These equations give the relationship between the tube inside and outside diameter in the heat exchanger and also distance between tubes where constraints are defined later to apply to optimization for the problem. It is useful to study effects of fins and tubes and their thermal resistance effects on the overall heat transfer. This is to determine if the fins are increasing or decreasing the heat transfer rate from the tubes to the PCM in the shell side.

Moreover the overall efficiency is then defined as follows [36]:

$$\eta_o = 1 - \frac{N_f A_f}{A_{tot}}\left(1 - \eta_f\right) \tag{7}$$

Here, η_f is the efficiency of a single fin. The fin's efficiency is unity when there is no fin. Considering the circular fin for the external surface, the fin efficiency is defined in equation (8) where I and K are modified Bessel functions of the first and second kind. In addition, C_2 and m are defined as follows:

$$\eta_f = \frac{C_2[K_1(mr_1)I_1(mr_{c2}) - I_1(mr_1)K_1(mr_{c2})]}{[I_0(mr_{r1})K_1(mr_{c2}) + K_0(mr_1)I_1(mr_{c2})]} \tag{8}$$

$$C_2 = \frac{2r}{m(r_{2c}^2 - r_1^2)} \tag{9}$$

$$m = \sqrt{\frac{2h_o}{k_w t}} \tag{10}$$

Here, h_i is the convection heat transfer coefficient on the tube side, estimated as follows [37]:

$$h_i = \frac{k_f}{d_i}\left(3.657 + \frac{0.0677\cdot(\mathrm{Re}\cdot\mathrm{Pr}\cdot d_i/L)^{1.33}}{1 + 0.1\cdot\mathrm{Pr}(\mathrm{Re}\cdot d_i/L)^{0.3}}\right) \quad \text{for} \quad \mathrm{Re} \le 2300 \tag{11}$$

$$h_i = \frac{k_f}{d_i}\left\{\frac{\frac{f}{2}\times(\mathrm{Re}-1000)\cdot\mathrm{Pr}}{1 + 12.7\cdot\sqrt{\frac{f}{2}}(\mathrm{Pr}^{0.67}-1)}\right\} \quad \text{for} \quad 2300 < \mathrm{Re} \le 10000 \tag{12}$$

where $f = (1.58\log(Re) - 3.28)^{-2}$

$$h_i = \frac{k_f}{d_i}\left\{\frac{\frac{f}{2}\times\mathrm{Re}\cdot\mathrm{Pr}}{1.07 + \frac{900}{\mathrm{Re}} - \frac{0.63}{1+10\mathrm{Pr}} + 12.7\cdot\sqrt{\frac{f}{2}}(\mathrm{Pr}^{0.67}-1)}\right\} \text{ for } \mathrm{Re} > 10000 \tag{13}$$

The pressure drop in the copper tubes and bundle can also be estimated from Equation (16) with f representing the friction factor on the tube side.

$$f = 0.00128 + 0.1143(\mathrm{Re})^{-0.311} \tag{14}$$

$$\mathrm{Re} = 4m/(\pi d_i \mu N) \tag{15}$$

$$\Delta P = 4NfLm^2 \Big/ \left(\rho\pi^2 d_i^2\right) \tag{16}$$

Furthermore, the outside convection heat transfer coefficient (h_o) estimated as follows [38]:

$$h_o = \frac{Nu \times k_f}{\Delta r_m} \tag{17}$$

Here, k_f and Δr_m are PCM conductivity and thickness of heat storage material which are related to the Nusselt number as follows [38]:

$$Nu = 0.28\left(\frac{\Delta r_m Ra}{L}\right)^{0.25} \quad \text{For} \quad Ra \ge 1000, \ \Delta r_m \le 0.006 \tag{18}$$

$$Nu = 1 \quad \text{For} \quad Ra < 1000, \quad \Delta r_m \le 0.006 \tag{19}$$

$$Nu = 0.133(Ra)^{0.326}\left(\frac{\Delta r_m}{L}\right)^{0.0686} \quad \text{For} \quad \Delta r_m > 0.006 \tag{20}$$

where Rayleigh number is defined as a function of Grashof and Prandtl numbers.

$$Ra = Gr \times \mathrm{Pr} \tag{21a}$$

$$Gr = \frac{g\beta(T_{h,i} - T_c)\Delta r_m^3}{\upsilon^2} \tag{21b}$$

Experimental data [39] for transient variations of the PCM radial temperature are used to determine the thickness of the PCM in the above calculations. The shell diameter is determined from the calculations for a tube bundle design of shell-and-tube heat exchangers [40]:

$$D_s = 0.637 p_t \sqrt{(\pi N_t) CL/CTP} \tag{22}$$

where p_t is pitch and CL is a tube layout constant that has a unit value for a 45° and 90° tube arrangement and 0.87 for 30° and 60° tube arrangements. Also, CTP is a tube count constant, which is 0.93, 0.9, and 0.85 for single pass, two passes and three passes of tubes, respectively.

3.2. Analysis of the PCM-CNT mixture

By mixing the nanotubes in the PCM, the effective properties will be changed. The predicted thermal conductivity of the mixture has been introduced in the design parameters of the heat exchanger. The effective thermal conductivity mainly depends on the direction of the nanotubes.

When the phase change material is used as storage media, the length of the heat storage system exceeds the limits. This is due to the main drawback of phase change materials which is a low thermal conductivity. The predicted length for this case will be presented in the following sections. In order to overcome this problem, nanoparticles are introduced to increase the thermal conductivity and rate of heat transfer in the PCM. This will lead to a more compact storage system which satisfies the objective function. Carbon Nanotubes and graphene nanoplatelets are considered as additives. For absorbed PCM in the foam, the following relation can be used to estimate the effective specific heat and thermal conductivity:

$$Cp_{\mathrm{eff}} = \frac{1}{m_{tot}} \times \sum m_i Cp_i = \frac{m_{pcm}}{m_{tot}} Cp_{pcm} + \frac{m_{CNT}}{m_{tot}} Cp_{CNT} \tag{23}$$

Here, the porosity (c) is defined as the volumetric ratio of PCM over the total available volume:

$$c = \frac{V_{pcm}}{V_{\text{tot}}} = \frac{V_{pcm}}{V_{pcm} + V_{cnt}} \tag{24}$$

$$Cp_{\text{eff}} = \frac{\rho_{pcm}}{\rho_{\text{tot}}} \times c \times C_{pcm} + \frac{\rho_{CNT}}{\rho_{\text{tot}}} \times (1-c) \times Cp_{CNT} \tag{25}$$

where K_{eff} and ρ_{eff} can be defined similarly in Equation (22). Based on the concentration equation (24), the effective thermal conductivity in series and parallel configurations is calculated by the following equations [41]:

$$k_{\text{eff},P} = \left(\frac{c}{k_{pcm}} + \frac{1-c}{k_{cnt}}\right)^{-1} \tag{26a}$$

$$\frac{k_{\text{eff}}}{k_{cnt,P}} = \left(c\frac{k_{cnt}}{k_{pcm}} + (1-c)\right)^{-1} \tag{26b}$$

$$k_{\text{eff},S} = ck_{pcm} + (1-c)k_{cnt} \tag{27a}$$

$$\frac{k_{\text{eff}}}{k_{cnt\,\text{series}}} = c\frac{k_{pcm}}{k_{cnt}} + (1-c) \tag{27b}$$

Note that the variations of effective thermal conductivity are studied in this paper for the practical concentration and carbon nanotubes probability of series arrangement.

3.3. Optimization with genetic algorithms

Evolutionary algorithms (EAs) are highly relevant for industrial applications, because of their ability to handle problems with non-linear constraints, multiple objectives, and dynamic components that frequently appear in real problems [42]. The genetic algorithm (GA) is an optimization technique based on natural genetics. Even though originally designed as simulators, GAs provide a robust optimization technique. The general concept of GAs could be described as follows. A random set of points within the optimization space is created by selection of points. These sets of points are then transformed into a new set. Moreover, this new set will contain extra points that are closer to the global optimum. The transformation procedure is based only on the information of optimality of each point in the set, consisting of simple string manipulations, and repeated several times.

The occupied volume is a main criterion in the heat exchanger design. The length of the heat exchanger has been defined as the objective function and design parameters are considered to be the number of tubes, tube inside and outside diameter, and shell diameter. One of the main advantages of GAs is their capability to use any desirable constraints in the optimization. Also, GAs usually find more than one near-optimal point in the optimization space, which provides more solution options for the optimization problem. The length of heat exchanger is considered an objective function. In order to minimize this objective function, five design parameters, namely, number of tubes, index of each tube, shell (tank) diameter, CNT concentration and CNT series probability are selected. The design parameters and their range of variation are shown in Table 1.

Due to the specific space limitations in vehicle applications, the maximum allowable tank diameter to be selected is considered to be 0.3 m. Moreover, the maximum allowable CNT concentration and series probability are chosen to be 10% and 0.2, respectively. At 9%, the mixture will resemble a semi-solid. Concentrations more than 10% are rarely reported in the literature. Tube schedules, outside diameter, tube thickness and tube fin length are listed in Table 2. In order to minimize the heat exchanger length, seven design parameters including number of tubes, index of each tube, shell (tank) diameter, CNT concentration and CNT series probability are selected. Tube schedules and corresponding tube outside diameter, tube thickness and tube fin length are listed in Table 3.

Table 1
Design parameters and their range of variation.

	Lower bound	Upper bound
Number of tubes	1	200
Index of tube	1	5
Tank diameter (m)	0	0.3
CNT concentration (%)	0	10
CNT series probability (%)	0	20

Table 2
Tube specification for the optimization (Data from Ref. [45].

Tube schedule number	3/16	1/4	5/16	3/8	1/2
Tube outside diameter (mm)	6.096	8.128	9.855	11.455	16.002
Tube thickness (mm)	0.752	0.762	0.889	0.889	1.575
Tube fin length (mm)	5.080	5.588	6.096	6.604	8.890

4. Results and discussion

Though inorganic materials have a high latent heat of fusion and their density is two times higher than organic materials, the incongruent melting and corrosion and toxicity properties make them unfavorable in applications. For instance, sodium hydroxide, as a salty hydrate PCM is a toxic and corrosive material. For eutectics, the main part of the compound is inorganic material which holds the same problems of inorganic materials in eutectics. For non-paraffin materials, like fatty acid, their high costs can be as high as 2 times other PCMs which is a disadvantage of this group of organic materials compared with paraffin organics. Iso-paraffins are not applicable to this study, because these PCMs have the disadvantage of temperature variations during freezing. This is in contrast with the assumption that constant temperature is needed to have effective thermal management in the battery. Normal-Octadecane is selected for the current study. Its melting point is around 29.5 °C, which makes it more suitable for the current application and for controlling the temperature. The disadvantage of low thermal conductivity can be improved by certain methods like encapsulation or embedding the PCM inside a graphite matrix and other methods.

In this study, two configurations for the carbon nanotubes are taken into consideration. If they are placed in a series configuration, the effective thermal conductivity increases significantly. On the other hand, the effective thermal conductivity will not have a significant increase when the nanotubes are placed in the parallel arrangement. Fig. 3 shows the variations of effective thermal conductivity for the parallel arrangement of the particles of carbon. This can be considered as the worst scenario. The label pointing to

Table 3
Soft copper tube specification for optimization.

Size (O.D.)	Outer diameter (mm)	Inner diameter (mm)	Wall thickness (mm)
1/8″	3.16	1.651	0.762
3/16″	4.76	3.2385	0.762
1/4″	6.35	4.826	0.762
5/16″	7.937	6.3119	0.8128
3/8″	9.525	7.8994	0.8128
1/2″	12.7	11.0744	0.8128

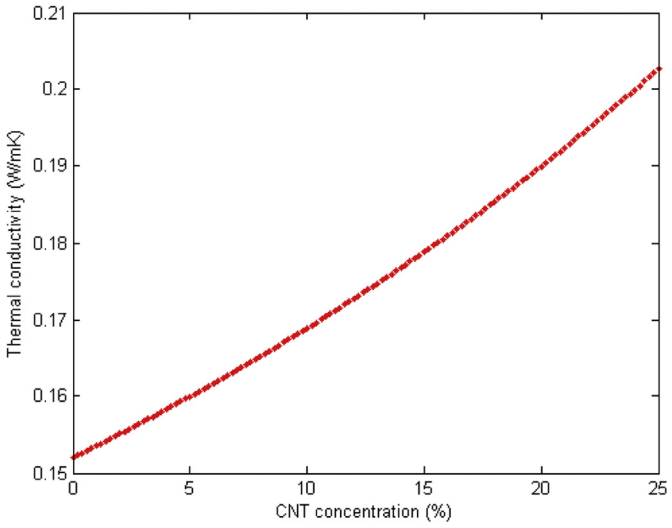

Fig. 3. Effect of CNT concentration on the thermal conductivity of the mixture in parallel configuration.

the zero concentration corresponds to an effective thermal conductivity ratio of $k_{\text{eff}}/k_{cnt,\text{P}} = 5.067 \times 10^{-5}$ where by considering a thermal conductivity of 3000 W m^{-1} K^{-1} for CNT, then $k_{\text{eff},P} = 5.067 \times 10^{-5} \times 3000 = 0.152$ W m^{-1} K^{-1}.

The value is the same as the thermal conductivity of a pure PCM. The best scenario corresponds to the case where the carbon nanotubes are set in series with the direction of the temperature gradient. On the other hand, the highest thermal conductivity is expected for a series configuration. From Fig. 4, for a 10% concentration for CNT, the effective thermal conductivity of a series configuration will be $K_{\text{eff}} = K_{\text{cnt}} \times 0.1 = 3000 \times 0.1 = 300$ W m^{-1} K^{-1}. The second approach is based on a probability for distribution of the CNTs. In this method, a weighting is given for the best (series) and worst (parallel) arrangements of CNTs in the mixture. If "P" is defined as the probability of a series arrangement (best case), then

$$k_{\text{mix}} = P \times k_{\text{eff},S} + (1-P)k_{\text{eff},P} \tag{28}$$

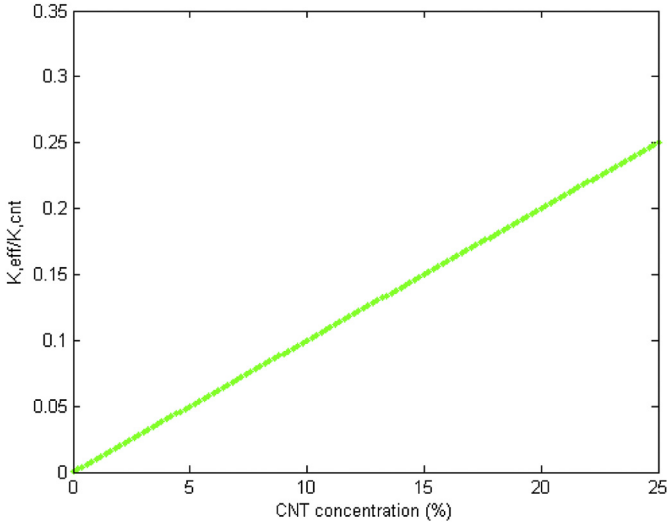

Fig. 4. Effective thermal conductivity of the PCM and Nanoparticles in series arrangement.

$$k_{\text{mix}} = P(c \times k_{pcm} + (1-c)k_{cnt}) + (1-P)\left(\frac{c}{k_{pcm}} + \frac{1-c}{k_{cnt}}\right)^{-1} \tag{29}$$

where c and series and parallel effective thermal conductivities are given in Equations (24), (26) and (27). Fig. 5 shows the effective thermal conductivity as a function of concentration and probability.

The operating conditions considered here for the heat exchanger are given as follows. The hot water with a minimum mass flow rate of 0.02 kg s^{-1} enters in the tube side as a hot stream. The PCM is placed in the shell side to absorb the minimum 300 W heat generated by the battery. The melting point of PCM is assumed to be 28.5 °C. The coolant is 50–50 water-ethylene glycol which leaves the tubes at 29.5 °C. Both finned and un-finned tube structures are considered in the straight tube. The genetic algorithm optimization is performed for 150 generations, using a search population size of $M = 100$ individuals, crossover probability of pc = 0.9, and gene mutation probability of pm = 0.035 for both cases (with and without finned tube). The results for the optimum length versus generation for both cases are shown in Fig. 6. The optimum values for the heat exchanger length are 32.95 cm and 41.09 cm respectively for the case without and with finned tubes. As a result, the application of the fin for tubes is not recommended in this case. The optimal design parameters for each case are listed in Table 4. The tube with a schedule number less than the 5/16 is not available in the market. As a result, the tubes with a smaller schedule number of 5/16 are omitted in the optimization process. By increasing the PCM thermal conductivity, the overall heat transfer coefficient increases, and as a result, the required heat transfer surface area decreases for specific heat duty. Consequently, by decreasing the heat transfer surface area, the length of tube and heat exchanger decreases.

This result is consistent with the experimental studies which show that the solidification time can be reduced by 20% by adding (less than 1%) multi-wall carbon nanotubes (MWCNT) to the PCM. Increased thermal conductivity results in the present study, directly leads to decreased solidification time in the storage system [43]. Also, other experimental studies for the thermal conductivity increase of paraffin-based nanocomposite PCMs shows an enhancement up to 164% at the loading of 5 wt.% of carbon nanoparticles [44]. The experimental study also indicates that thermal conductivity enhancement depends mainly on the size and shape of the nanoparticles which is consistent with the present study. The "the shape" of the nanoparticles is defined as a nanoparticles series configuration in the mixture.

The variations of heat exchanger length versus effective thermal conductivity of the PCM are shown in Fig. 7. It is observed that by increasing of the effective thermal conductivity, the heat exchanger length decreases. The variation of optimum heat exchanger length and shell diameter in terms of the variation of the standard tube (with specific inner and outer diameter) are depicted in Table 5. Other specifications of the copper tubes can be seen in this Table. It is concluded that by increasing the tube diameter, both heat exchanger length and shell diameter increase. As a result, the minimum available tube diameter in the market is suitable in this case. Essentially, by increasing the tube diameter, the Reynolds number decreases, and as a result, the inner convection heat transfer coefficient and overall heat transfer coefficient decrease. By decreasing the overall heat transfer coefficient, the total heat transfer surface area (length of tubes) should increase, which is consistent with Ref. [34].

The genetic algorithm is employed for different copper tube sizes. Based on the results, the available standard tubes in the

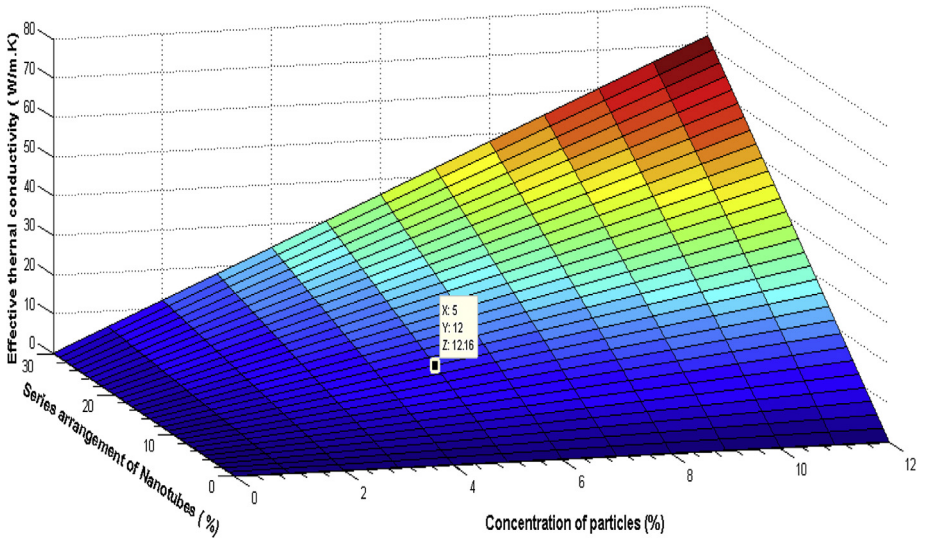

Fig. 5. Thermal conductivity as a function of concentration and probability.

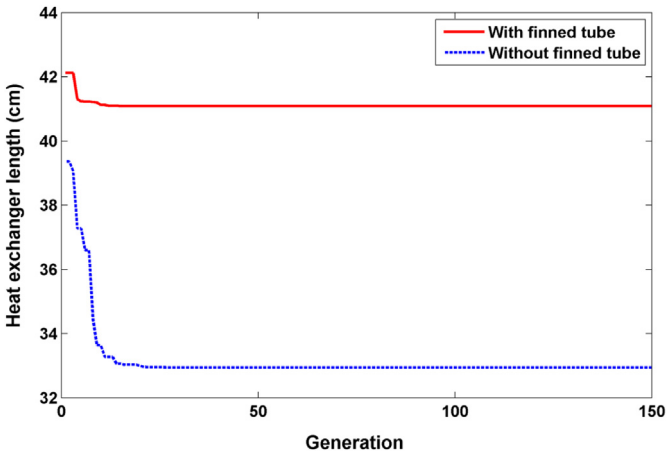

Fig. 6. Convergence of objective function versus number of generation for both cases.

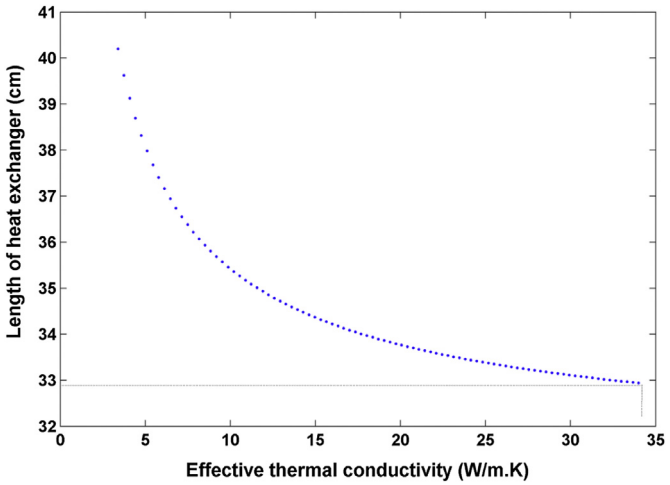

Fig. 7. Variation on length of heat exchanger versus effective thermal conductivity of the PCM.

market are considered as design outputs. Figs. 8 and 9 illustrate these variations for the tubes respectively. By increasing the tube index, the tube inside and outside dimensions are also increased. It is determined that, by increasing the tube diameter, both L/d_i and D/d_o decrease. Fig. 10 shows the variations of L/d_i and D/d_o versus the variations of tube index. It is deduced that the rate of increment in tube inside and outside diameter is higher than the rate of increment in the tube length and shell diameter as seen from Fig. 10. The variation of optimum value of tube length versus tube inner diameter for various heat loads is shown in Fig. 11. The optimum tube length increases by increasing the tube inner diameter with a constant slope. Furthermore, the optimum value of tube length increases by an increase in the rate of heat transfer flow (HTF).

Table 4
Comparison of optimum results in cases including with and without finned tubes.

Type	Tube type	Length of H.X (cm)	Tank diameter (cm)	Number of tubes	CNT concentration (%)	CNT series probability
Finned	5/16	41.09	33.97	47	10	20
No fin	5/16	32.95	27.56	62	8.6	19.7

The variation of "L/d" versus Reynolds number and rate of heat transfer for various tube diameters is shown in Fig. 12. It can be seen that a higher value of heat transfer needs a higher value of Reynolds number and L/d. A variation of heat exchanger length versus CNT series probability and CNT concentration at the optimum point is shown in Fig. 13. The values of heat exchanger length which cannot satisfy the problem constrains are not illustrated in these figures. It also can be seen that the heat exchanger length decreases by

Table 5
Variations of optimum heat exchanger length and shell diameter versus tube diameter.

Tube size	Index	d_i (mm)	d_o (mm)	L (mm)	D (mm)
1/16.	1	1.14	1.59	16.4	13.7
1/8.	2	1.65	3.18	16.72	13.93
3/16.	3	3.23	4.75	20.8	17.53
1/4.	4	4.83	6.35	24.7	20.74
5/16.	5	6.30	7.93	28.41	23.79
3/8.	6	7.90	9.53	32.1	26.77
7/16.	7	9.49	11.11	35.33	29.51
1/2.	8	11.13	12.70	39.33	32.64

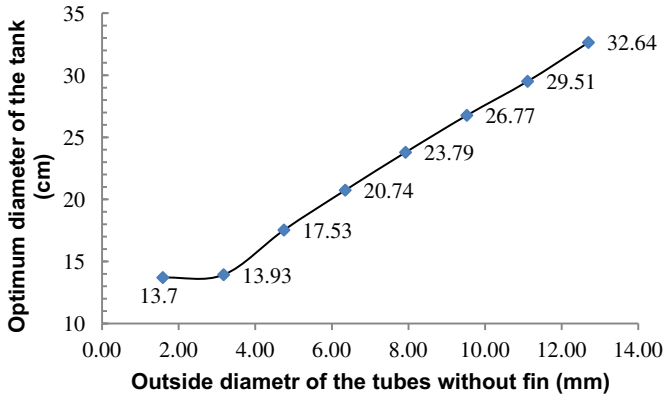

Fig. 8. Variation of optimum shell (tank) diameter versus tube outside diameter in the case without fin.

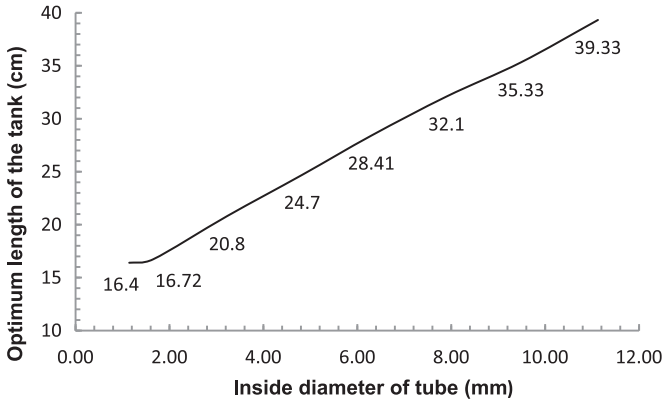

Fig. 9. Variation of optimum tube length versus tube inside diameter in the case without fin.

increasing both CNT probability and concentration. The maximum length is taken at the minimum possible CNT probability and concentration. Furthermore, in addition at the zero CNT probability and concentration (pure PCM) there is no optimum design to satisfy the constraint. The optimum heat exchanger length has been illustrated as a function of CNT concentration and series configuration probability in Fig. 14. Contours reveal the regions that cannot satisfy the constraints. The bottom left corner corresponds to the pure PCM which provides the lengths that fail to meet the

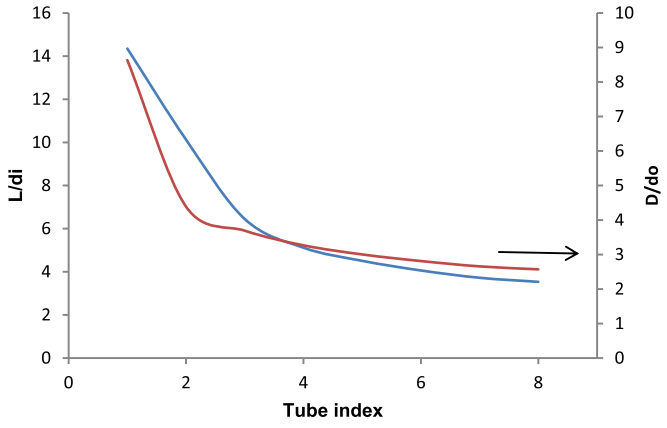

Fig. 10. Variation of L/di and D/do versus the tube index.

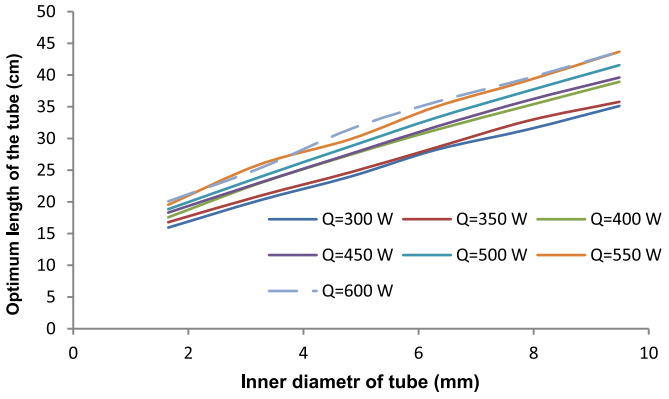

Fig. 11. Variation of optimum value of tube length versus tube inner diameter for various rates of heat transfer.

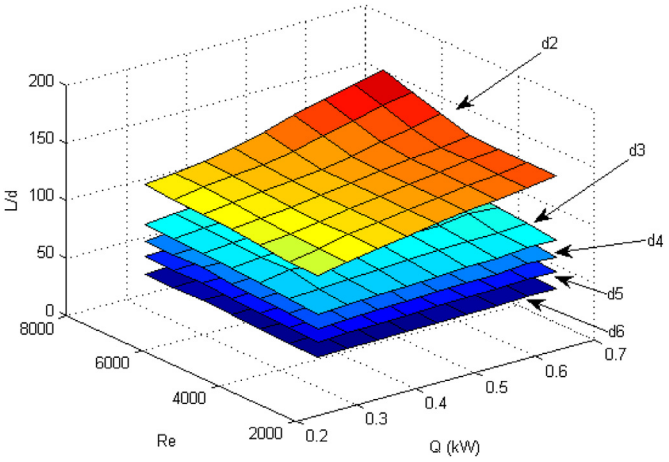

Fig. 12. Dependency of Re, rate of heat transfer and L/d for various tube diameters.

requirements and satisfy the constraint. The optimum length has been obtained for different values of heat generation (Q) and various mass flow rates which give different Reynolds numbers. Once all the available tubes, starting from 1/16" diameter up to 1" diameter, are investigated with respect to the variable mass flow rates and heat transfer rates (300 W–600 W) to be handled

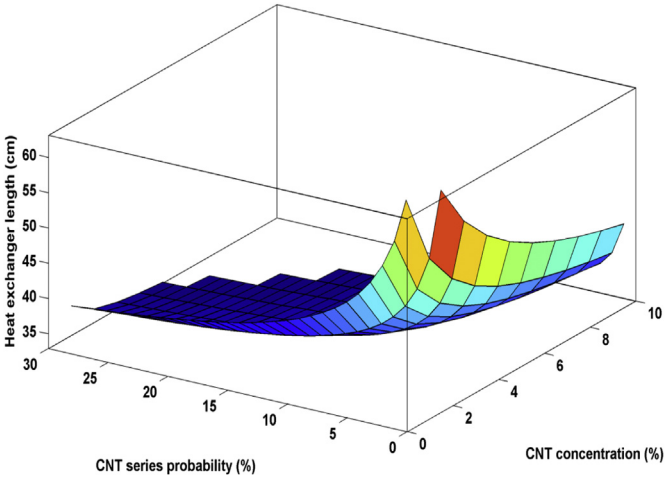

Fig. 13. Variation of heat exchanger length versus CNT series probability and CNT concentration at optimum point.

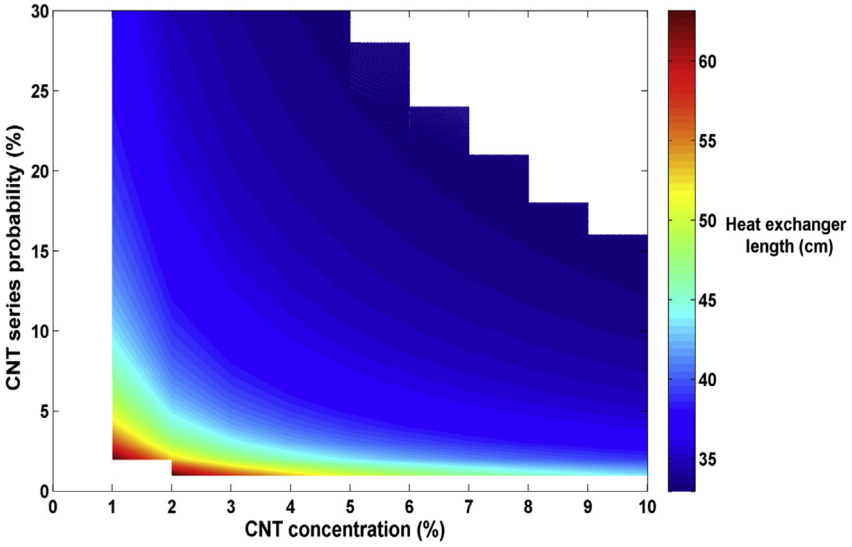

Fig. 14. Contour of heat exchanger length versus CNT series probability and CNT concentration at optimum point.

through the heat exchanger, the following relationship fits the set of diagrams with the least error,

$$\frac{LD}{d^2} = 471.55 + \mathrm{Re}\left(1 + 381.28 \times \frac{Q}{L_{\mathrm{melt}}}\left(1 + \frac{\mathrm{Re}}{893}\right)\right) \tag{30}$$

where "L" and "D" are the optimum length and diameter of the tank. L_{melt} is the latent heat of fusion for the phase change material. The Re number is calculated based on the total mass flow rate $D_H = 4H/P$, where D_H is the hydraulic diameter. If "N" is the number of tubes in the heat exchanger, then

$$D_H = d\sqrt{N} \tag{31}$$

$$R_e = \frac{4\dot{m}_{\mathrm{total}}}{\mu\pi D_H} \tag{32}$$

It can be seen that the heat exchanger length decreases by an increase of both CNT probability and concentration and the maximum length is taken at the minimum possible CNT probability and concentration. In addition, at the zero CNT probability and concentration (pure PCM), there is no optimum design to satisfy the constraint as the case for straight copper tubes. Based on the optimization results, the heat exchanger is manufactured as shown in Fig. 2b). Copper tube sizes are 5/16".

5. Conclusions

A design and optimization of a latent heat thermal energy storage system is developed for passive thermal management of an electric vehicle. Considering the optimum charging and discharging time, shell and tube heat exchanger geometries are considered in straight copper tubes. Due to specific restrictions in terms of available space in the vehicle, the length of the heat exchanger length is taken as the objective function and genetic algorithm is applied to find the optimum values of design parameters. In addition, specific constraints regarding the heat exchanger shell diameter are considered. As the main drawback of PCMs, pure PCM also has a very small thermal conductivity of 0.15 W m^{-1} K^{-1}. An evolutionary-based optimization method of genetic algorithms is employed to minimize the length of the heat exchanger as the objective function. Subsequently, the optimum length of heat exchanger becomes too large to be practically employed in the thermal management of the vehicle. In order to solve this issue, the CNT (carbon Nanotube) or Graphene Nanoplatelets are added to the PCM to improve the thermal conductivity of the mixture and consequently, the heat exchanger length. In order to minimize this objective, five design parameters, namely, number of tubes, index of each tube, shell (tank) diameter, CNT concentration and CNT series probability, are selected. The optimization method is applied for both tube configurations including the straight bare and finned tubes. The concluding remarks of the current study are summarized as follows:

- The following correlation is established for calculating the length and diameter of the heat exchanger for thermal management of electric vehicles: $LD/d^2 = 471.55 + Re\ (1 + 381.28 \times Q/L_{melt}(1 + Re/893))$ for a range of heat transfer rates from 300 W to 600 W.
- Smaller tube diameters minimize the heat exchanger length and 5/16 inch diameter tubes are selected as the optimum diameter. The corresponding pressure drop is less than 2 kPa which is within that which can be compensated by the operating pump.
- By increasing the tube diameter, both heat exchanger aspect ratio including L/d_i and D/d_o decrease.
- *n*-Octadecane (n-$C_{18}H_{38}$) as normal paraffin has been selected for the current study. This organic PCM has advantageous properties such as congruent melt, ignorable sub cooling due to self-nucleating ability and compatibility with other materials (container material).
- The pure phase change material cannot give the required compactness to the heat exchanger (length will not be applicable).
- By increasing both CNT concentration and CNT series probability, the optimum value of heat exchanger decreases.
- The application of a fined tube in the case of a straight tube leads to the higher heat exchanger length due to more heat transfer resistance and geometrical constraints.

Acknowledgments

The financial support from Automotive Partnerships Canada (APC) (grant number APCPJ 386787-09) and the Natural Sciences and Engineering Research Council of Canada (NSERC) is gratefully

acknowledged. The authors also wish to thank the Canadian Regional Engineering Center (CREC) for their support during the research. Furthermore, the authors thank Dr. Greg Rohrauer for his valuable assistance during the research.

Nomenclature

A	area (m^2)
c	volumetric concentration of CNT
C_p	specific heat (kJ kg K^{-1})
D	heat exchanger diameter (m)
d	tube diameter (m)
f	friction factor
h	convection heat transfer coefficient
Gr	Grashof number
k	thermal conductivity (W m K^{-1})
L	heat exchanger length (m)
N	number of tubes
Nu	Nusselt number
P	pressure (Pa)
P	probability of CNT in series configuration
Pr	Prandtl number
$\dot{Q}$	heat transfer rate (kW)
R	resistance (Ω)
Ra	Rayleigh number
Re	Reynolds number
s	distance between the fins
T	temperature (K or °C)
U	overall heat transfer coefficient
V	velocity (m s^{-1})
Δr_m	thickness of heat storage material (m)
ΔT_{lm}	logarithmic mean temperature (K)

Greek symbols

Δ	change in variable
β	thermal expansion coefficient (1/K)
η_o	overall efficiency of the fin
υ	kinematic viscosity (m^2 s^{-1})
ρ	density (kg m^{-3})

Subscripts

b	base
c	cold
f	fin
h	hot
i	internal, inside
o	outside
P	parallel
q	heat
S	series
t	fin thickness
tot	total
w	wall

Acronyms

CNT	carbon nanotube
CENG	compressed expanded natural graphite
EV	electric vehicle
HEV	hybrid electric vehicle
HTF	heat transfer fluid
ICE	internal combustion engine
LHTES	latent heat thermal energy storage
LMTD	logarithmic mean temperature difference
PCM	phase change material
TMS	thermal management system

References

[1] D. Streimikiene, T. Baležentis, L. Baležentienė, Renew. Sustain. Energy Rev. 20 (2013) 611–618.
[2] Q. Wang, P. Ping, X. Zhao, G. Chu, J. Son, C. Chan, J. Power Sources 208 (2012) 210–224.
[3] A.A. Pesaran, S. Burch, M. Keyser, An approach for designing thermal management systems for electric and hybrid vehicle battery packs, in: Proceedings of the 4th Vehicle Thermal Management Systems, 1999, pp. 24–27.
[4] Y. Yang, X. Hu, D. Qing, F. Chen, Energies 6 (5) (2013) 2709–2725.
[5] M.R. Giuliano, A.K. Prasad, S.G. Advani, J. Power Sources 216 (2012) 345–352.
[6] J. Lee, K. Choi, N. Yao, C. Christianson, J. Electrochem. Soc. 133 (7) (1986) 1286–1291.
[7] R. Sabbah, R. Kizilel, J.R. Selman, S. Al-Hallaj, J. Power Sources 182 (2) (2008) 630–638.
[8] L. Fan, J. Khodadadi, A. Pesaran, J. Power Sources 238 (2013) 301–312.
[9] M.-S. Wu, K. Liu, Y.Y. Wang, C.C. Wan, J. Power Sources 109 (1) (2002) 160–166.
[10] X. Duan, G.F. Naterer, Int. J. Heat Mass Transf. 53 (23) (2010) 5176–5182.
[11] M. Ramandi, M.,I. Dincer, G.F. Naterer, Heat Mass Transf. 47 (7) (2011) 777–788.
[12] N. Javani, I. Dincer, G.F. Naterer, B.S. Yilbas, Int. J. Heat Mass Transf. 72 (2014) 690–703.
[13] F.P. Brito, J. Martins, L.M. Goncalves, R. Sousa, SAE Int. J. Passeng. Cars Electron. Electr. Syst. 5 (2) (2012).
[14] N. Javani, I. Dincer, G.F. Naterer, Energy 46 (2012) 109–116.
[15] F. Agyenim, N. Hewitt, O. Eames, M. Smyth, Renew. Sustain. Energy Rev. 14 (2) (2010) 615–628.
[16] M. Esen, A. Durmuş, A. Durmu&scedil, Sol. Energy 62 (1) (1998) 19–28.
[17] J. Prakash, H. Garg, G. Datta, Energy Convers. Manage. 25 (1) (1985) 51–56.
[18] C. Bellecci, M. Conti, Int. J. Heat Mass Transf. 36 (8) (1993) 2157–2163.
[19] M. Akgün, O. Aydın, K. Kaygusuz, Appl. Therm. Eng. 28 (5) (2008) 405–413.
[20] A. Trp, K. Lenic, B. Frankovic, Appl. Therm. Eng. 26 (16) (2006) 1830–1839.
[21] A. Sharma, V.V. Tyagi, C.R. Chen, D. Buddhi, Renew. Sustain. Energy Rev. 13 (2) (2009) 318–345.
[22] M.M. Farid, A.M. khudhair, S.K. Rzack, S. Al-Hallaj, Energy Convers. Manage. 45 (9) (2004) 1597–1615.
[23] B. Zalba, J.M. Marin, L.F. Cabeza, H. Mehling, Appl. Therm. Eng. 23 (3) (2003) 251–283.
[24] S. Sharma, K. Sagara, Int. J. Green. Energy 2 (1) (2005) 1–56.
[25] A. Abhat, Sol. Energy 30 (4) (1983) 313–332.
[26] S. Jegadheeswaran, S.D. Pohekar, Renew. Sustain. Energy Rev. 13 (9) (2009) 2225–2244.
[27] N. Javani, I. Dincer, G.F. Naterer, B.S. Yilbas, Appl. Therm. Eng. 64 (1–2) (2014) 471–482.
[28] H. Hamut, I. Dincer, G.F. Naterer, Int. J. Energy Res. 37 (1) (2013) 1–12.
[29] J. Xu, T.S. Fisher, Int. J. Heat Mass Transf. 49 (9) (2006) 1658–1666.
[30] Y. Xu, Y. Zhang, E. Suhir, X. Wang, J. Appl. Phys. 100 (7) (2006) 074302.
[31] N. Vyshak, G. Jilani, Energy Convers. Manage. 48 (7) (2007) 2161–2168.
[32] X. Py, R. Olives, S. Mauran, Int. J. Heat Mass Transf. 44 (14) (2001) 2727–2737.
[33] K. Foli, T. Okabe, M. Olhofer, Y. Jin, B. Senhoff, Int. J. Heat Mass Transf. 49 (5) (2006) 1090–1099.
[34] S. Sanaye, H. Hajabdollahi, Appl. Therm. Eng. 30 (14) (2010) 1937–1945.
[35] H. Hajabdollahi, P. Ahmadi, I. Dincer, J. Thermophys. Heat Transf. 25 (3) (2011) 424–431.
[36] R.K. Shah, P. Sekulic, Fundamental of Heat Exchanger Design, John Wiley & Sons, Inc., 2003.
[37] A.C. Caputo, P.M. Pelagagge, P. Salini, Appl. Therm. Eng. 28 (10) (2008) 1151–1159.
[38] H. El-Dessouky, F. Al-Juwayhel, Energy Convers. Manage. 38 (6) (1997) 601–617.
[39] H. Ettouney, H. El-Dessouky, E. Al-Kandari, Ind. Eng. Chem. Res. 43 (17) (2004) 5350–5357.
[40] S. Kakac, Liu, Heat Exchangers Selection Rating, and Thermal Design, CRC Press, New York, 2000.
[41] M.T. Strauss, R.L. Pober, J. Appl. Phys. 100 (8) (2006), 084328–084328-9.
[42] D. Goldberg. Genetic Algorithms in Optimization, Search and Machine Learning. Addison Wesley, New York. Eiben AE, Smith JE (2003) Introduction to Evolutionary Computing. Springer. Jacq J, Roux C (1995) Registration of non-segmented images using a genetic algorithm. Lecture notes in computer science, 1989. 905: p. 205–211.
[43] V. Kumaresan, P. Chandrasekaran, Maitreyee Nanda, A.K. Maini, R. Velraj, Int. J. Refrig. 36 (6) (2013) 1641–1647.
[44] L.-W. Fan, X. Fang, X. Wang, Y. Zeng, Y.Q. Xiao, Z.-T. Yu, X. Xu, Y.-C. Hu, K.-F. Cen, Appl. Energy 110 (2013) 163–172.
[45] Integral Hihg-Finned Copper Tube. Dayco Industries, Mira Loma, CA, USA.